Transient Response Analysis for Fault Detection and Pipeline Wall Condition Assessment in Field Water Transmission and Distribution Pipelines and Networks

by

Mark Leslie Stephens

February 2008

A Thesis Submitted for the Degree of Doctor of Philosophy

School of Civil and Environmental Engineering
The University of Adelaide, SA 5005
South Australia

Chapter 8

Transient Model and Roughness Calibration for Transmission Pipelines

---

The development of increasingly complex forward transient models for the calibration of pipe roughness, incorporating combinations of quasi-steady friction, unsteady friction and entrained air algorithms, is presented in this chapter. A conceptual model incorporating "viscous" damping, as outlined in Chapter 5, is also presented. Each proposed model is calibrated to measured responses using inverse analysis and the feasibility of fitted physical parameters is assessed. The objective is to identify a complex forward transient model that can account for non-fault related dispersion and damping with sufficient accuracy to permit successful transient response analysis and/or Inverse Transient Analysis (ITA) for fault detection and/or pipe wall condition assessment. In this context, the calibration of the pipe roughness is part of the pipe wall condition assessment. Because of limitations to the scope of this research model development and roughness calibration will only be performed for the Hanson Transmission Pipeline (HTP).

8.1 Roughness calibration using inverse transients

Calibration can be performed using a quasi-steady friction transient model and inverse analysis to identify roughness values along a pipeline or within a network. However, given the influence of unsteady friction, entrained air and mechanical dispersion and damping on the response of field pipelines, the calibrated roughness values may not represent the physical roughness of the pipeline. It is necessary to develop and calibrate a quasi-steady friction model in order to assess the potential importance of other phenomena that cause dispersion and damping. Calibration is then repeated using increasingly complex transient models, including combinations of unsteady

friction, entrained air and mechanical mechanisms, to determine whether any improvement relative to the results obtained using the traditional quasi-steady friction (QSF) model can be achieved.

8.2 Quasi-steady friction model

A quasi-steady friction model (QSF), based on the forward transient model introduced in Chapter 7, has been used to calibrate for the roughness along the Hanson Transmission Pipeline (HTP) and offtake branch to the Burra township pump station. Limited CCTV camera inspection has been undertaken along 300m of the HTP between chainages 8800m and 9100m. This footage enabled the roughness along the HTP to be estimated as approximately 2mm.

8.2.1 Results of calibration using quasi-steady friction model

Table 8-1 shows the results of the calibration using a quasi-steady friction (QSF) model. The average fitted roughness values, for no-leak tests 1 and 2, were 6.98mm and 3.04mm, for the Hanson Transmission Pipeline (HTP) and offtake branch, respectively. The value for the HTP varies significantly from the CCTV camera determined roughness of approximately 2mm. The short length of the CCTV camera footage makes extrapolating an estimate from it unreliable. That said, a calibrated roughness value for the HTP of approximately 7mm, while plausible, was higher than expected.

Table 8-1 - Fitted main pipeline and offtake branch roughness values obtained following calibration using a QSF model

Fitted Parameter	TEST 1		TEST 2		Average Value of Mean μ
	Mean μ	Standard Deviation σ	Mean μ	Standard Deviation σ	
ε_{HTP}	0.706e-02	0.763e-04	0.690e-02	0.774e-04	0.698e-02
ε_{Branch}	0.297e-02	0.287e-03	0.311e-02	0.285e-03	0.304e-02
Objective Function	12.390		12.373		12.382

Figures 8-1 and 8-2 show, for test 1, that the QSF model gives a poor fit between the measured and calibrated responses at both measurement stations. Figures 8-3 and 8-4 show the measured response lagging the predicted response over the first 100s. This lag is indicative of either the presence of entrained air and/or dispersion caused by mechanical motion and vibration. The objective functions for tests 1 and 2, following the inverse analysis and calibration, are shown in Table 8-1 and confirm that the model could not be accurately calibrated despite the determination of optimal roughness parameters.

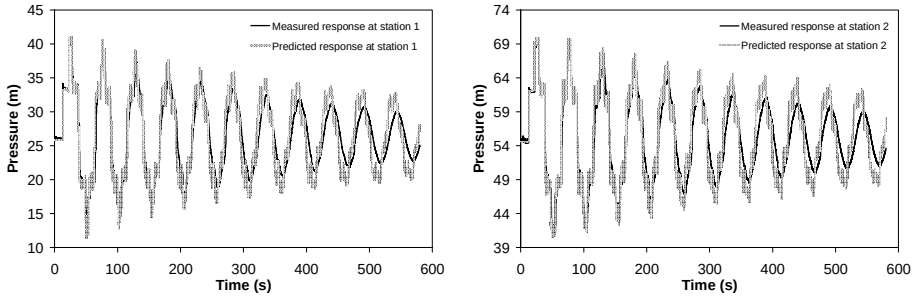

Figures 8-1 and 8-2 – Comparison of measured and calibrated responses, over 580s, when a QSF model is used, at stations 1 and 2, respectively

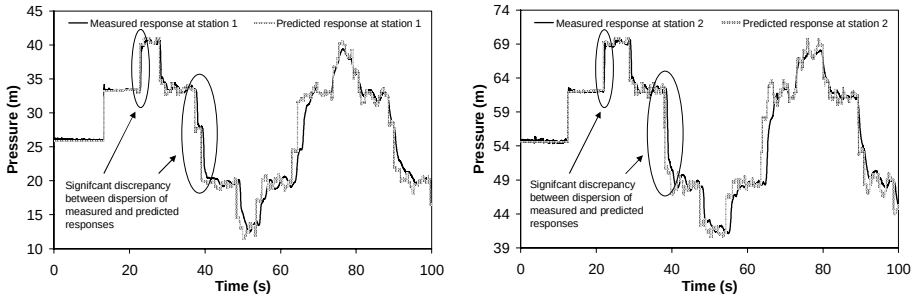

Figures 8-3 and 8-4 – Comparison of measured and calibrated responses, over 100s, when a QSF model is used, at stations 1 and 2, respectively

8.2.2 Regression results for quasi-steady friction model

Examining the measured versus predicted response and standardised residual versus time gives an insight into the performance of the quasi-steady friction (QSF) model

after calibration to the measured responses for test 1. Figures 8-5 and 8-6 show the relationship between the measured and predicted responses for test 1 at measurement stations 1 and 2, respectively. The average coefficient of determination is 83.2% for both tests.

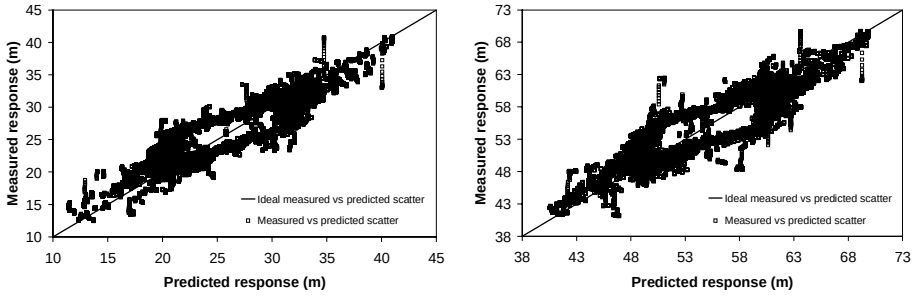

Figures 8-5 and 8-6 – Measured versus predicted plots for test 1, at stations 1 and 2, respectively

Figures 8-7 and 8-8 show the standardised residual plotted against time for test 1 at stations 1 and 2, respectively. Two significant observations can be made. Firstly, a lag between the measured and predicted response is clearly discernable over, in particular, the initial 100s of the response. Figures 8-9 and 8-10 below show the residual plotted against time over the initial 100s and confirm that there are numerous spikes in the residual that are caused by the measured response lagging the predicted response in time.

The second significant observation, apparent in Figures 8-7 and 8-8, is that the ability of the QSF model to capture the dispersion and damping during the later stages of the response progressively deteriorates leaving a structured cyclic pattern in the residual corresponding to an increasing discrepancy between the measured and predicted responses. In the context of Inverse Transient Analysis (ITA) for leak detection, it is not possible to use the damping information within the measured responses, related to a leak, if the QSF model is unable to adequately replicate non-leak related damping. It is therefore important that a calibration model be identified that can adequately replicate the dispersion and damping that occurs in the Hanson Transmission Pipeline (HTP), when no-leak is present, over all time scales.

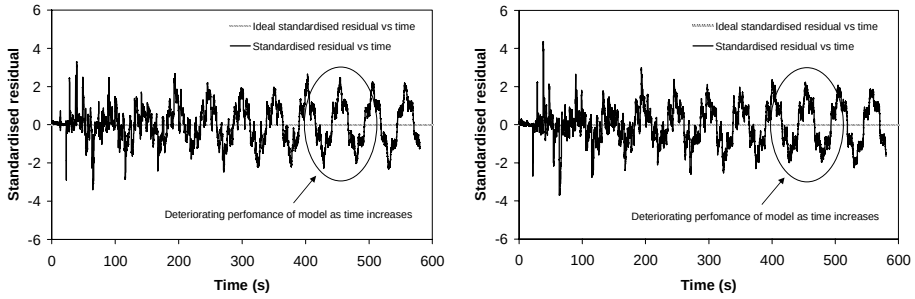

Figures 8-7 and 8-8 - Standardised residual versus time plots for test 1, over 580s, at stations 1 and 2, respectively

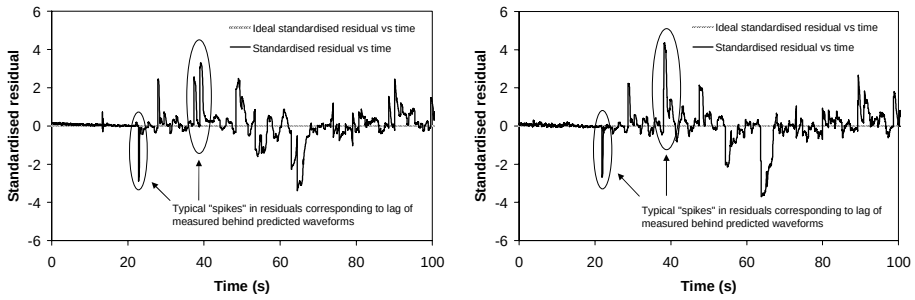

Figures 8-9 and 8-10 - Standardised residual versus time plots for test 1, over 100s, at stations 1 and 2, respectively

Table 8-2 shows the correlation, for test 1, between the roughness values fitted for the HTP and the offtake branch. The two roughness parameters are highly correlated and variations in either during the regression analysis are not independent. This is a consequence of the way in which the two parameters are used in the QSF model to establish initial steady conditions and then abstract a quasi-steady friction loss after the transient has been initiated.

Given the lack of fit achieved after calibrating the QSF model, the structural inability of the model to replicate the longer term damping in the HTP and the high correlation between the roughness parameters for the main pipeline and offtake branch, the QSF calibration model is considered generally inadequate. This conclusion is significant

for researchers, notably Tang et al. (1999), who have published transient pipe roughness calibration results using quasi-steady friction models in field networks.

Table 8-2 - Correlation of main pipeline and offtake branch roughness obtained for the Hanson Transmission Pipeline for QSF calibration model

Parameter	ε_{HTP}	$\varepsilon_{AC\ Branch}$
ε_{HTP}	1.000	0.995
$\varepsilon_{AC\ Branch}$	0.995	1.000

8.3 Unsteady friction model

8.3.1 Results of calibration using unsteady friction model

Table 8-3 shows the results of the calibration using an unsteady friction (UF) model. The test flows were in the transition turbulent section of the Moody diagram. Consequently, the unsteady friction calculations were performed using the equations applicable to turbulent flow conditions in a rough pipe (given the anticipated roughness was at least 2mm based on the available CCTV camera footage). An efficient recursive approximation of the weighting function for turbulent rough pipe unsteady friction, developed by Vitkovsky et al. (2004), was implemented as described in Appendix E and this facilitated efficient inverse analysis using the NLFIT suite of programs.

The average fitted roughness values, for no-leak tests 1 and 2, were 6.51mm and 3.98mm, for the Hanson Transmission Pipeline (HTP) and offtake branch, respectively. The results for tests 1 and 2 vary slightly. However, the average values are of the same order as obtained using the quasi-steady friction (QSF) model. Once again, while the calibrated roughness values are plausible they are higher than expected. The anticipated roughness value of 2mm, based on the direct CCTV camera investigation, is supported by steady pressure measurements elaborated below. This suggests that the calibrated roughness value obtained using the UF model is greater than the physical value for the main pipeline.

Table 8-3 - Fitted main pipeline and offtake branch roughness values obtained for the Hanson Transmission Pipeline using an UF calibration model

Fitted Parameter	TEST 1		TEST 2		Average Value of Mean μ
	Mean μ	Standard Deviation σ	Mean μ	Standard Deviation σ	
ε_{HTP}	0.655e-02	0.395e-05	0.646e-02	0.405e-05	0.651e-02
ε_{Branch}	0.379e-02	0.118e-04	0.416e-02	0.106e-03	0.398e-02
Objective Function	1.656		1.652		1.654

Significant outcomes emerge from the inverse calibration performed using turbulent rough pipe unsteady friction. Figures 8-11 and 8-12 show that the fit between the measured and predicted responses is significantly improved, relative to the results obtained using the QSF model, for test 1, at stations 1 and 2, respectively. An incorrect interpretation of this result is that the neglect of unsteady friction is the sole explanation for the discrepancies observed when using the QSF model and that when approximately the same roughness values are used, and unsteady friction is included, the discrepancies are correctly accounted for. This conclusion is made more appealing because the objective functions following the calibration of excessively high roughness values are low.

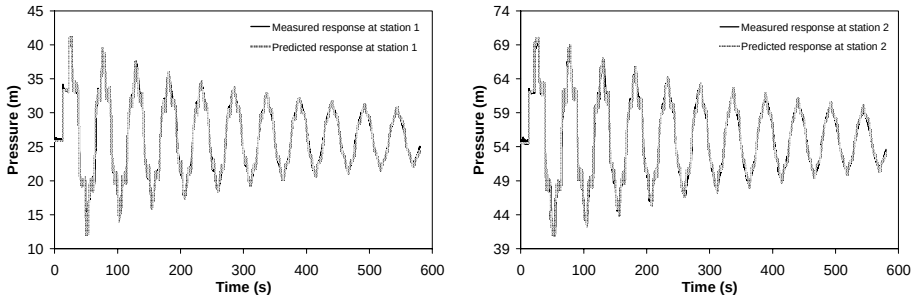

Figures 8-11 and 8-12 – Comparison of measured and calibrated responses for the no-leak case over 580s, at stations 1 and 2, respectively

The problem is that the calibrated roughness value is significantly higher than the known roughness derived from direct CCTV investigation and steady state

comparisons elaborated below. This is a very important warning that particular mechanisms, in this case unsteady friction, should not be applied inappropriately to draw incorrect conclusions regarding the roughness of a pipeline. Minimisation of objective function has dominated the thinking of researchers using inverse transients. However, as shown above, blind use of the objective function as the sole criteria for assessing model performance can lead to misleading conclusions regarding which phenomena are responsible for observed dispersion and damping and the accuracy, and physical relevance, of calibrated parameters.

The suspicion that the UF model does not explain all the phenomena affecting the measured response of the HTP is confirmed when the comparison between the measured and predicted responses over 100s is considered. Figures 8-13 and 8-14 show that, as for the results obtained using the QSF model, the dispersion in the measured response is not correctly predicted.

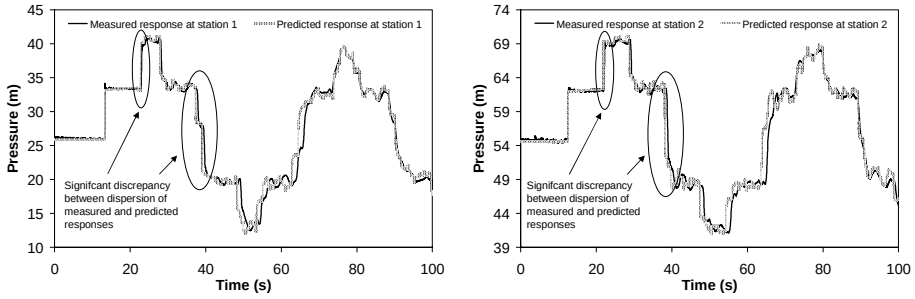

Figures 8-13 and 8-14 – Comparison of measured and calibrated responses for the no-leak case over 100s, at stations 1 and 2, respectively

8.3.2 Regression results for unsteady friction model

While unsteady friction does not explain the discrepancies between the measured and predicted dispersion, it nevertheless accounts for a significant proportion of the damping and leads to an overall improvement in the predicted responses. Figures 8-15 and 8-16 show the relationship between the measured and predicted responses for test 1 at measurement stations 1 and 2, respectively. Relative to the results for the quasi-steady friction (QSF) model, there is considerably less scatter. The average coefficient

of determination is 97.3% for both tests. Spikes corresponding to discrepancies between the measured and predicted responses are observed where the unsteady friction (UF) model has failed to replicate dispersion observed in the measured responses.

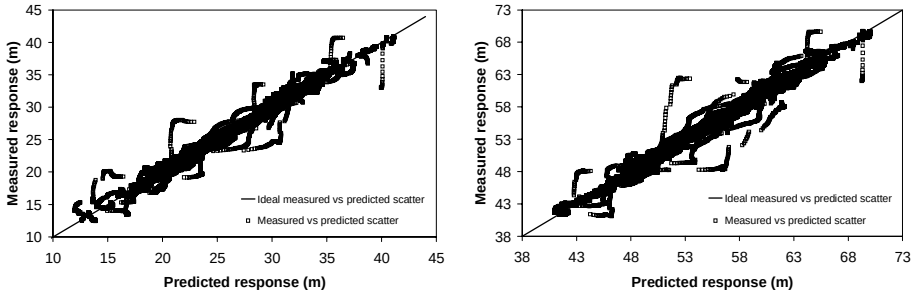

Figures 8-15 and 8-16 – Measured versus predicted plots for test 1 at stations 1 and 2, respectively

Figures 8-17 and 8-18 show the standardised residual plotted against time for test 1 at stations 1 and 2, respectively. A lag between the measured and predicted response is clearly discernable over, in particular, the initial 100s of the response. Figures 8-19 and 8-20 below show the residual plotted against time over the initial 100s and confirm that there are numerous spikes in the residual that are caused by the measured response lagging the predicted response in time.

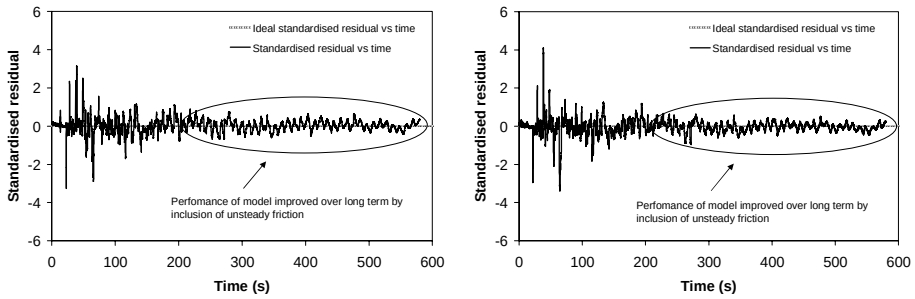

Figures 8-17 and 8-18 - Standardised residual versus time plots obtained for test 1, over 580s, at stations 1 and 2, respectively

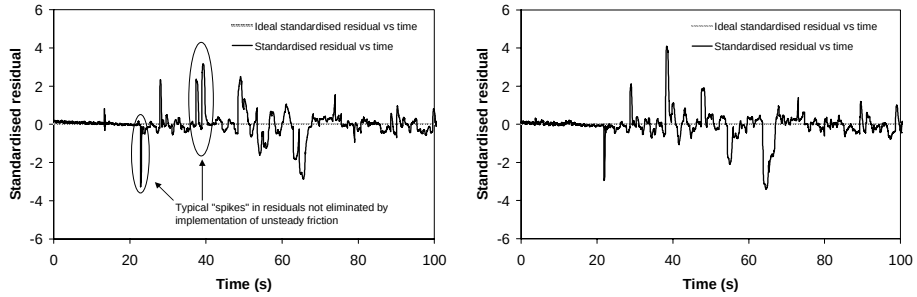

Figures 8-19 and 8-20 - Standardised residual versus time plots for test 1, over 100s, at stations 1 and 2, respectively

In contrast to the results obtained using the QSF model, the UF model replicates the majority of the damping occurring over the later stages of the response. The deteriorating cyclic pattern in the standardised residual, obtained when applying the QSF model, is largely eliminated. In the context of Inverse Transient Analysis (ITA) for leak detection, this improvement increases the likelihood that the leak related damping information in the response will be able to be isolated. That said, significant damping that is not related to unsteady friction remains unaccounted for, particularly if the known roughness value of 2mm is used, and the effect of entrained air and/or mechanical dispersion and damping may obscure leak related damping information. Furthermore, the spikes in the standardised residual, caused by dispersion in the measured response that is not predicted, persist for both the QSF and UF models.

Table 8-4 shows the correlation, for test 1, between the roughness values fitted for the Hanson Transmission Pipeline (HTP) and the offtake branch. In contrast to the results for the QSF model, the two roughness parameters are not correlated and variations in either during the regression analysis are relatively independent. The lack of correlation is a consequence of the way in which the roughness value is used in the turbulent rough pipe calculation for unsteady friction in the HTP and offtake branch.

Despite the improved fit achieved after calibrating the unsteady friction (UF) model, and the enhanced ability of the model to substantially replicate the longer term damping in the HTP, and the lack of correlation between the two roughness parameters, the UF model remains inadequate for the purpose of pipe roughness

calibration. The calibrated roughness values exceed the known values (determined from a mix of CCTV camera investigation and steady state calibration). The accuracy with which the UF model predicts the measured responses is reduced when a known (lower) roughness value is used.

Table 8-4 - Correlation of main pipeline and offtake branch roughness obtained for the Hanson Transmission Pipeline for UF calibration model

Parameter	ε_{HTP}	$\varepsilon_{AC\ Branch}$
ε_{HTP}	1.000	-0.278
$\varepsilon_{AC\ Branch}$	-0.278	1.000

8.4 Unsteady friction with entrained air model

The possibility that entrained air is present in the Hanson Transmission Pipeline (HTP) cannot be discounted. A discrete gas cavity model (DGCM) is used in the following section to include distributed entrained air along the length of the HTP. Regression diagnostics, after the calibration of the roughness of the HTP (and offtake branch) and volume of distributed entrained air, are examined to determine whether the observed dispersion is correctly predicted and/or the level of structural model error is reduced. Unsteady friction calculations are performed using the efficient recursive approximation developed by Vitkovsky et al. (2004).

8.4.1 Calibration for roughness and entrained air over 580 seconds

Table 8-5 shows the results of the calibration for tests 1 and 2, using long term measured responses (i.e., over a time scale of 580s), when a discrete gas cavity with unsteady friction (DGCUF) model is applied to include the effect of unsteady friction and any entrained air. Given there was no prior information regarding the likely distribution of entrained air, discrete gas cavities were included for each computational section along the Hanson Transmission Pipeline (HTP). The average calibrated air pocket size was 0.00054L or 0.0000083% for both tests. The average fitted roughness values for the HTP and offtake branch, for both tests, were 2.75mm

and 3.38mm, respectively. Importantly, the fitted roughness values are significantly less than those obtained when using the UF model without distributed air pockets. Furthermore, the calibrated roughness value approximately matches the known value.

The effect of such a small calibrated volume of entrained air upon the calibrated pipeline roughness values illustrates the interdependency between mechanisms that predominately disperse and damp (i.e., entrained air and unsteady friction) in the context of least squares regression parameter calibration. In the case of entrained air, it is critical that its presence be either confirmed, and the likely quantity identified, or discounted. If not, the erroneous omission or exclusion of entrained air will potentially invalidate roughness calibration performed using quasi-steady friction (QSF) or unsteady friction (UF) models.

Table 8-5 - Fitted distributed air pocket size and main pipeline and offtake branch roughness values obtained for the HTP using a DGCUF calibration model

Fitted Parameter	TEST 1		TEST 2		Average Value of Mean μ
	Mean μ	Standard Deviation σ	Mean μ	Standard Deviation σ	
ε_{HTP}	0.278e-02	0.102e-05	0.272e-02	0.111e-05	0.275e-02
ε_{Branch}	0.341e-02	0.323e-05	0.335e-02	0.330e-05	0.338e-02
$V_{air\ pock}$	0.532e-06	0.207e-08	0.550e-06	0.209e-08	0.541e-06
Objective Function	2.284		2.286		2.285

While there has been an improvement in terms of the fitted roughness of the HTP, the fit between the measured and calibrated responses has deteriorated with the objective function increasing from an average value of 1.654 to 2.285 for the UF and DGCUF models, respectively. If objective function values were relied upon as the sole criteria for assessing goodness of fit then this result would indicate that the UF model is superior and that the fitted volume for each distributed air pocket is incorrect. However, given information indicating that the roughness of the HTP is approximately 2mm, and given information that the quantity of entrained air along the HTP is unlikely to be less than 0.54mL per sub-segment (refer to Appendix N), the

hypothesis that the UF model over-calibrates the roughness to compensate for dispersion and damping related to other phenomena appears to be correct.

The calibrated volume for each distributed air pocket is plausible given that the velocities in the 24 hours prior to the tests were generally sufficient to move any free air to air valves and each air valve was flushed prior to the tests (with little free air reported). The fitted quantity of free air of 0.54mL translates to approximately 1000 bubbles of free air (1mm diameter is a typical bubble size for entrained air) per sub-pipe segment. This is a low quantity of free air. It is suspected that interdependency between the effects of entrained air and unsteady friction may have contributed to a marginal underestimation of the quantity of entrained air.

The initial assessment of the effect of entrained air, presented in Chapter 7, indicated that while 0.0005% gave a reasonable approximation of the observed dispersion over the short term, it caused excessive dispersion of the predicted response over the long term. In contrast, Figures 8-21 and 8-22 show that a reasonable match between the measured and predicted responses is obtained when the DGCUF model is calibrated over the long term.

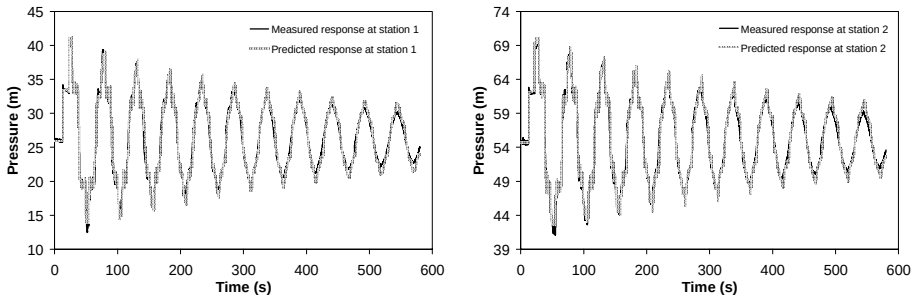

Figures 8-21 and 8-22 – Comparison of measured and predicted responses for test 1 obtained using the DGCUF model calibrated over 580s (shown over 580s)

However, Figures 8-23 and 8-24 show that the dispersion observed over the initial stages of the measured response is not correctly predicted for the calibrated volume of entrained air. This problem is investigated by calibrating the DGCUF model over the

initial stages of the transient response to determine whether a different quantity of entrained air is obtained (below).

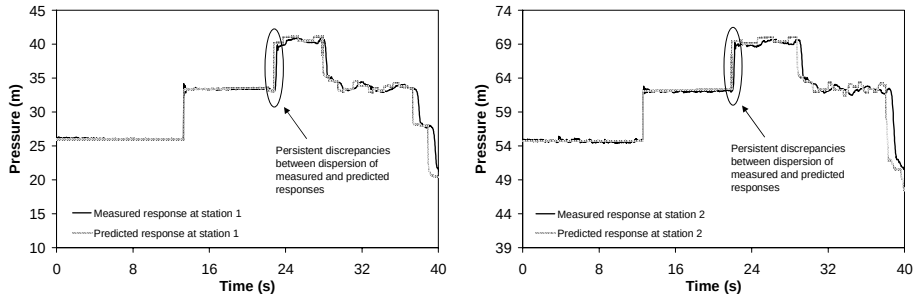

Figures 8-23 and 8-24 – Comparison of measured and predicted responses for test 1 obtained using the DGCUF model calibrated over 580s (shown over 40s)

8.4.2 Calibration for roughness and entrained air over 2L/a seconds

Table 8-6 shows the results of the calibration for tests 1 and 2, using short term measured responses, when a discrete gas cavity with unsteady friction (DGCUF) model is applied to include the effect of entrained air. The calibration was performed using the first 38.1s of the measured responses. This time comprised 12.5s at the initial steady condition and an additional 25.6s, corresponding to a period of 2L/a, after the transient was induced. The average fitted distributed air pocket size was 0.02L or 0.00031% for both tests.

The average fitted roughness values for the Hanson Transmission Pipeline (HTP) and offtake branch, for both tests, were 3.09mm and 6.08mm, respectively. The fitted roughness values were marginally less than those obtained when using the unsteady friction (UF) model without distributed air pockets. This again confirms that small quantities of air can have a significant effect upon model calibration. However, the fitted roughness values are close to those obtained when using the UF model and significantly greater than those obtained for the calibration using the long term responses.

Table 8-6 - Fitted distributed air pocket size and main pipeline and offtake branch roughness values obtained using a DGCUF model calibrated over the short term

Fitted Parameter	TEST 1		TEST 2		Average Value of Mean μ
	Mean μ	Standard Deviation σ	Mean μ	Standard Deviation σ	
ε_{HTP}	0.296e-02	0.441e-05	0.321e-02	0.410e-04	0.309e-02
ε_{Branch}	0.599e-02	0.313e-03	0.616e-02	0.388e-03	0.608e-02
$V_{air\ pock}$	0.199e-04	0.269e-06	0.200e-04	0.268e-06	0.200e-04
Objective Function	0.178		0.179		0.179

Interestingly, the average fitted distributed air pocket size is approximately 37 times greater than that obtained for the calibration using the long term responses. The calibrated volume of entrained air, and its distribution along the HTP, should remain relatively invariant and the similarity between the measured responses for tests 1 and 2 indicates that there was no significant change in the quantity or distribution of entrained air along the HTP.

Figures 8-25 and 8-26 show that the calibration using the short term measured responses successfully replicates the observed dispersion over the short term. However, as shown in Figures 8-27 and 8-28, the volume for each distributed air pocket calibrated using the short term response is too large and excessive long term dispersion occurs. The inconsistency between the results of the long and short term calibrations suggests that calibration should not be performed over the short term.

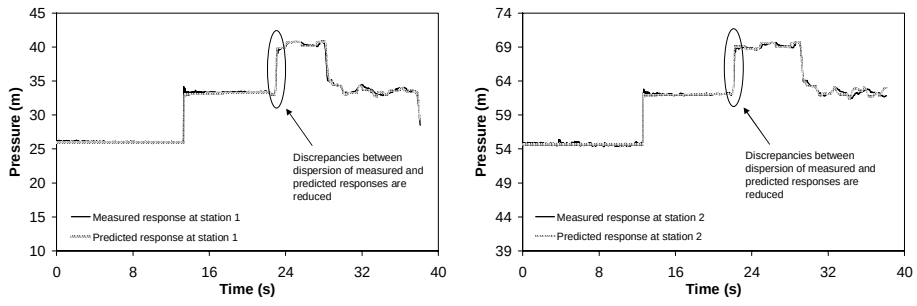

Figures 8-25 and 8-26 – Comparison of measured and predicted responses for test 1 obtained using the DGCUF model calibrated over 40s (shown over 40s)

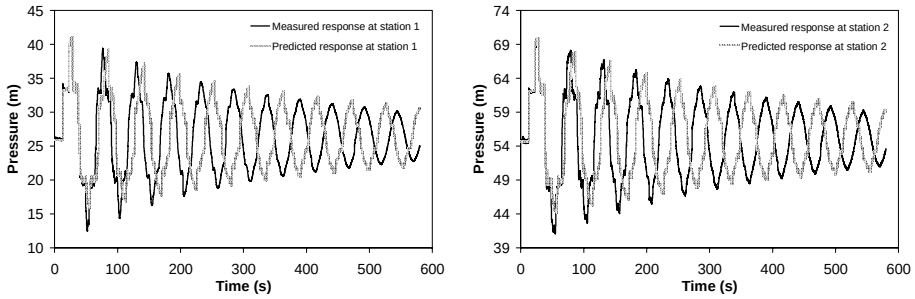

Figures 8-27 and 8-28 – Comparison of measured and predicted responses for test 1 obtained using the DGCUF model calibrated over 40s (shown over 580s)

This conundrum can only be explained, in the context of the possibility of entrained air, if the volume of air reduces (i.e., goes into solution) during the transient. Such behaviour is unlikely for the transients induced in the HTP. This means that some other phenomena must be responsible for the observed dispersion over the initial stages, and possibly the entire duration, of the measured transient responses.

8.4.3 Regression results presented over the short term

Figures 8-29 and 8-30 show the relationship between the measured and predicted responses for test 1, at measurement station 1, illustrated over the short term, for calibrations performed with the discrete gas cavity with unsteady friction (DGCUF) model. The calibrations have been performed using long and short term measured responses, respectively. The time scale is limited to 40s for the results obtained when using the long term calibration so that a comparison can be made with the results obtained when using the short term calibration. The average coefficients of determination are 96.0% and 99.6% using the percentage of entrained air for the long and short term calibrations, respectively. Figure 8-29 has spikes where the measured dispersion is not correctly predicted by the model calibrated over the long term.

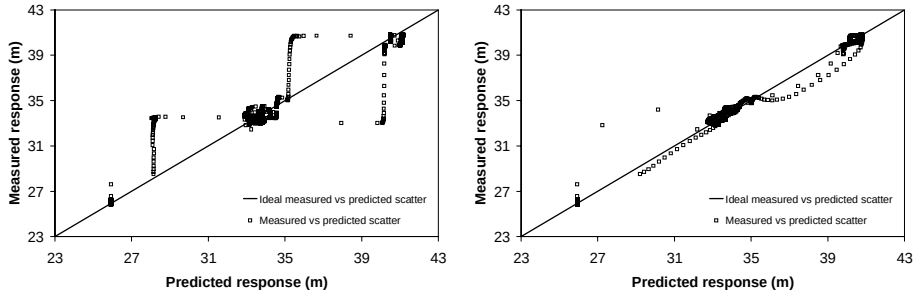

Figures 8-29 and 8-30 – Measured versus predicted plots obtained using the DGCUF model, with long and short term calibrations, respectively (shown over 40s)

Figures 8-31 and 8-32 show the standardised residual plotted against time, determined over the short term, for test 1, at measurement station 1, for calibrations to long and short term measured responses, respectively. Figure 8-31 shows that the long term calibration does not accurately predict the dispersion in the short term measured response. Figure 8-32 shows that the short term calibration does not completely eliminate discrepancies (particularly for reflections from the offtake branch).

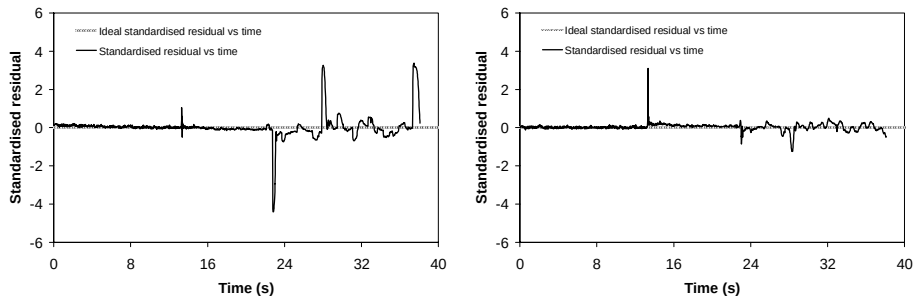

Figures 8-31 and 8-32 - Standardised residual versus time plots obtained using the DGCUF model, with long and short term calibrations, respectively (shown over 40s)

8.4.4 Regression results presented over the long term

Figures 8-33 and 8-34 show the relationship between the measured and predicted responses for test 1, at measurement station 1, determined over the long term, for calibrations, using the discrete gas cavity with unsteady friction (DGCUF) model, to long and short term measured responses, respectively. The average coefficients of

determination are 95.9% and 0.8% using the percentage of air determined for the long and short term calibrations, respectively. Figure 8-33 contains spikes because short term dispersion in the measured response is not correctly predicted. Figure 8-34 shows a complete failure of the model when the percentage of entrained air calibrated to the short term response is used for long term analysis.

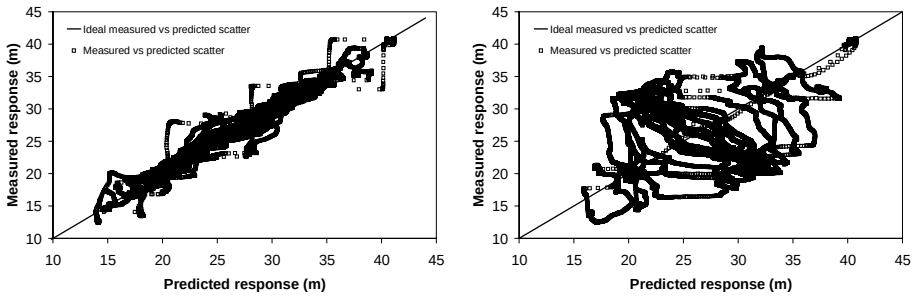

Figures 8-33 and 8-34 – Measured versus predicted plots obtained using the DGCUF model, with long and short term calibrations, respectively (shown over 580s)

Figures 8-35 and 8-36 show the standardised residual plotted against time, determined over the long term, for test 1, at measurement station 1, for calibrations to long and short term measured responses, respectively. Figure 8-35 shows persistent spikes, corresponding to a failure to model dispersion over the initial stages of the transient, and a persistent cyclical error over the long term. In contrast, the cyclical structure in Figure 8-36 indicates that the results from the short term calibration over predict the long term dispersion. Furthermore, the size of the cyclical error varies as the predicted response moves in and out of phase with the measured response.

While the long term dispersion is better predicted using the long term calibration, the calibrated percentage of entrained air is small. The quantity of entrained air calibrated over the short term gives rise to excessive dispersion over the long term predicted response. Overall, it is thought that the calibrated percentage of entrained air obtained following the long term calibration is likely to be representative of the “true” quantity of entrained air and that mechanical dispersion and damping, rather than unsteady friction or entrained air, is responsible for the observed dispersion, and residual damping, in the measured responses.

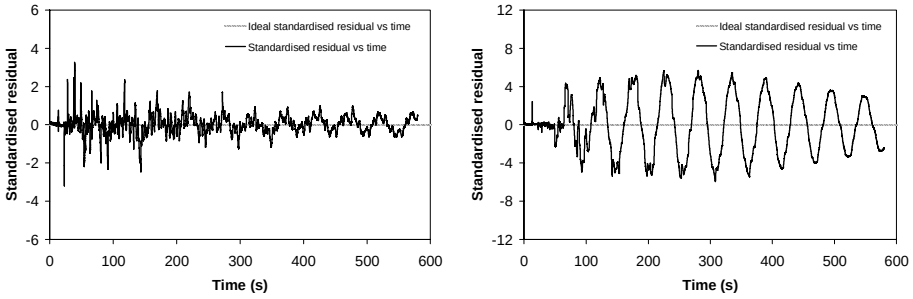

Figures 8-35 and 8-36 – Standardised residual versus time plots obtained using the DGCUF model, with long and short term calibrations, respectively (shown over 580s)

8.4.5 Parameter correlations for long and short term calibrations

Table 8-7 shows the correlations, when calibrating to the long term measured response for test 1, between the roughness values for both the Hanson Transmission Pipeline (HTP) and offtake branch and the size of the distributed air pockets. The two roughness parameters are not correlated. Furthermore, the roughness parameters are not correlated with the parameter for the size of the distributed air pocket.

Table 8-7 - Correlation of HTP and offtake branch roughness, and distributed air pocket volume, for calibration of DGCUF model over long term

Parameter	ε_{HTP}	$\varepsilon_{AC\ Branch}$	$V_{airpock}$
ε_{HTP}	1.000	0.435	-0.368
$\varepsilon_{AC\ Branch}$	0.435	1.000	0.480
$V_{airpock}$	-0.368	0.480	1.000

Table 8-8 shows the correlations, when calibrating to the short term measured response for test 1, between the roughness values for both the HTP and offtake branch and the size of the distributed air pocket. The two roughness parameters are only moderately correlated. However, the parameters for the roughness of the offtake branch and the size of the distributed air pocket are highly correlated. This is a curious

result and may indicate that both parameters have the potential to significantly affect the level of dispersion, over the short term, in the predicted response.

Table 8-8 - Correlation of HTP and offtake branch roughness, and distributed air pocket volume, for calibration of DGCUF model over short term

Parameter	ε_{HTP}	$\varepsilon_{AC\ Branch}$	$V_{airpock}$
ε_{HTP}	1.000	-0.784	0.830
$\varepsilon_{AC\ Branch}$	-0.784	1.000	-0.992
$V_{airpock}$	0.830	-0.992	1.000

Given the inconsistency between the calibrated percentage of air, depending on whether the long or short term measured response is used, and the improbability that free air returns to solution during the transient event, the presence of a significant quantity of entrained air cannot explain the dispersion observed in the measured responses for the HTP. That said, there are likely to be many other potential pipeline calibration scenarios where entrained air will be present in more significant quantities. The approach outlined above may assist in the calibration of such pipelines.

8.5 Unsteady friction with “viscous” damping model

8.5.1 Rationale supporting the use of a “viscous” calibration model

Field transmission pipelines (in particular, aboveground pipelines) have complex restraint conditions. As described in Chapter 5, the Hanson Transmission Pipeline (HTP) is supported by concrete saddles at an average spacing of 10m and restrained by concrete collar rings at an average spacing of 75m. Both lateral and longitudinal motion and vibration are feasible and the degree of support and restraint provided by the saddles and collars varies. In addition, Figure 8-37 shows that the Hanson Transmission Pipeline (HTP) has 22 locations where it deviates from above to below ground (i.e., to form gullets under road crossings). Most of these points are at the location of vehicular crossings. However, gullets have also been constructed at the upstream tank outlet, two cross-connection chambers, two in-line valve chambers, the

offtake to the Burra township pump station and at the insertion probe flow measurement station. These locations along the HTP act to provide significant longitudinal and lateral restraint in addition to the saddle supports and collar restraints previously identified.

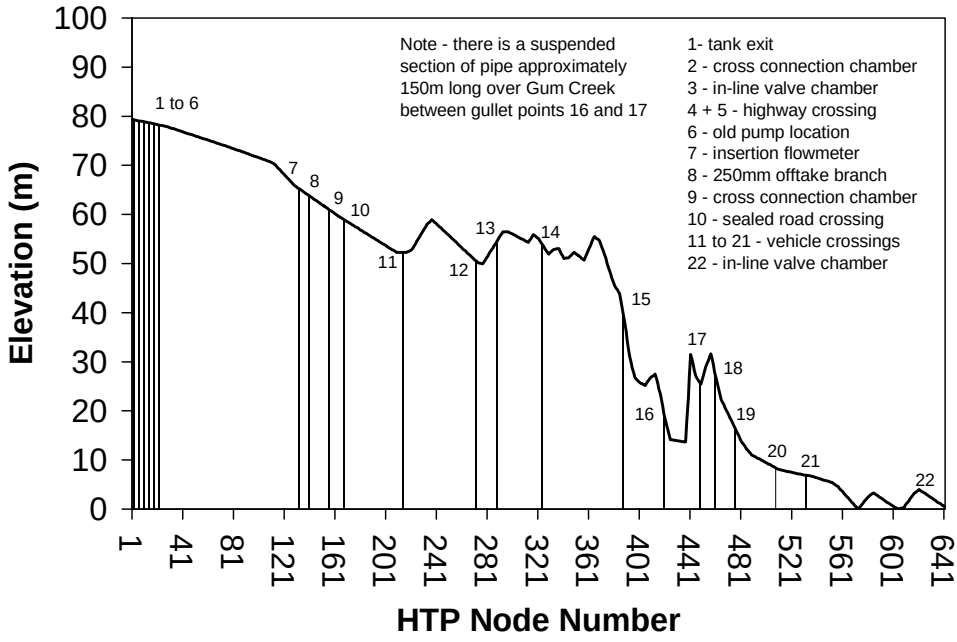

Figure 8-37 – Locations of underground sections along the Hanson Transmission Pipeline (gullets) with description of associated restraining structure

Based on the experimental findings of Budny et al. (1991), it is probable that the saddle supports, collar restraints, buried gullets, and, in the case of the HTP, the buried offtake branch with flexible joints, permit varying degrees of mechanical motion and vibration. It appears likely that flexural and shear waves form, as the pipeline moves or vibrates between restraints, and that these waves are responsible for the bulk of the observed dispersion and transfer energy to the pipeline restraints. This conclusion is supported by the fact that the inertial effects predicted by Skalak (1956), as described in Chapter 7, do not account for the bulk of the observed dispersion. It is also supported by the measured accelerations, for a large transmission pipeline parallel to the Morgan Transmission Pipeline (MTP), presented in Chapter 7.

The formation of flexural and shear waves from proliferating reflections at points of restraint are not accounted for in the Fluid Structure Interaction (FSI) models developed by Skalak (1956) and Budny et al. (1991), which incorporate equations relating fluid pressure, axial velocity, axial pipe stress and axial pipe velocity in a Method of Characteristics (MOC) scheme. The author has conducted further investigation, outside the scope of this research, into more complex FSI models that include equations for flexure, shear and torsion. However, none of these models are capable of reproducing the dispersion and damping caused by variable mechanical motion and vibration at pipeline restraints. This explains the development of the "viscous" damping mechanism by Budny et al. (1991).

Complex FSI models are not applied in this research because they are incapable of replicating the dispersion and damping caused by mechanical motion and vibration. Furthermore, as Williams (1977) suggested, the detailed physical information required by such models is not practically available even for laboratory apparatus. Instead, a conceptual forward transient model, based on the "viscous" damping mechanism presented in Chapter 5, will be used to account, on average, for mechanical dispersion and damping.

8.5.2 Configuration of a conceptual Kelvin-Voigt model

Kelvin-Voigt mechanical models are commonly applied to replicate time dependent strain relaxation in the walls of plastic pipes. However, viscoelastic models have also been applied to predict the response of pipelines subject to external dynamic loads and the interaction of pipes with surrounding soils (the behaviour of which can also be described as viscoelastic). Furthermore, the behaviour of flexible joints can be replicated using viscoelastic or "viscous" damping. The configuration of a typical Kelvin-Voigt mechanical element is illustrated in Figure 8-38 (where the components have been previously defined in Chapter 5). The elastic component of the viscoelastic mechanism is represented by the spring shown before the parallel spring and dashpot (with elastic stiffness E_0).

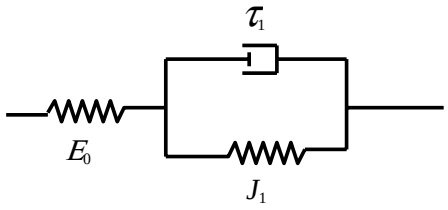

Figure 8-38 – A one-element Kelvin-Voigt mechanical viscoelastic model

For a pipeline subject to a transient, the wave speed of the pipeline represents this elastic spring stiffness. The "viscous" component of the mechanism comprises the spring and dashpot in parallel. Parameter J_1 is known as the compliance of the creep deformation spring and is equal to the reciprocal of the elastic spring stiffness E_1. Parameter τ_1 is known as the retardation time of the dashpot and is equal to the reciprocal of the viscosity of the dashpot μ_1. These parameters will be calibrated to replicate the mechanical dispersion and damping affecting the Hanson Transmission Pipeline (HTP).

The conceptual model presented in this chapter uses Kelvin-Voigt mechanisms to replicate the influence of saddle supports, collar restraints, buried in-line valve and cross-connection chambers, gullets along the HTP and to replicate the influence of the buried offtake branch with flexible joints. The Kelvin-Voigt elements are applied uniformly at each node along the HTP and the buried branch. Figure 8-39 shows the idealised distribution of the Kelvin-Voigt mechanical elements.

In addition to the roughness along the HTP and offtake branch, Kelvin-Voigt parameters J_{HTP}, τ_{HTP}, $J_{\text{AC Branch}}$ and $\tau_{\text{AC Branch}}$, characterising creep compliance functions for the HTP and offtake branch, will be calibrated (a total of 6 parameters need to be calibrated). The effects of unsteady friction are also modelled. Hence, the model has been labelled the unsteady friction and "viscous" Hanson pipeline and offtake branch (UFVHOB) model.

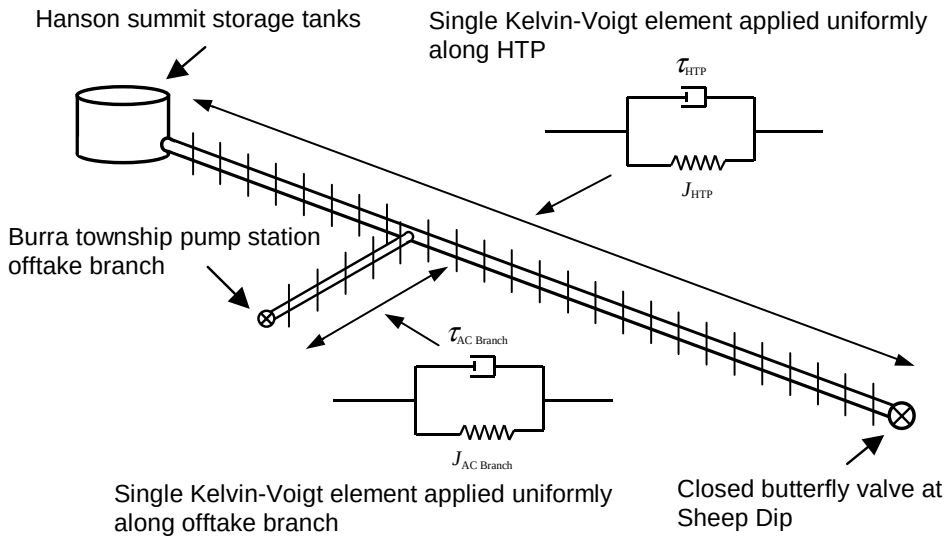

Figure 8-39 – Schematic of a conceptual viscous calibration model for the HTP

8.5.3 Results of calibration of UFVHOB model over long term

Table 8-9 shows the results of the calibration for tests 1 and 2, using long term measured responses, when the unsteady friction with a uniformly distributed "viscous" effect along the Hanson Transmission Pipeline (HTP) and offtake branch (UFVHOB) model is applied. The average fitted roughness values, for tests 1 and 2, are 5.22mm and 4.15mm for the HTP and offtake branch, respectively. These values are less than those obtained for the quasi-steady friction (QSF) and unsteady friction (UF) models but significantly greater than the known value inferred from the CCTV camera investigation and steady state tests.

Figure 8-40 shows the comparison of the compliance function curves for the HTP and offtake branch. The "viscous" damping is greater along the offtake branch, per unit length, and contributes more rapidly to the calibrated response, relative to the effect along the HTP. The compliance function curve derived using the calibrated J_{HTP} and τ_{HTP} parameters has a less significant damping effect, per unit length, and is slow acting (i.e., the full creep values do not apply until after time 16s). That said, the

cumulative effect of the calibrated "viscous" dispersion and damping along the main pipeline is significantly greater than that along the offtake branch.

Table 8-9 - Fitted HTP and offtake branch roughness values, and "viscous" parameters, obtained by calibrating the UFVHOB model over the long term

Fitted Parameter	TEST 1		TEST 2		Average Value of Mean μ
	Mean μ	Standard Deviation σ	Mean μ	Standard Deviation σ	
J_{HTP}	0.202e-13	0.234e-13	0.280e-13	0.205e-13	0.241e-13
τ_{HTP}	7.592	0.477e-01	6.178	0.246	6.885
$J_{ACBranch}$	0.163e-10	0.475e-12	0.142e-10	0.361e-12	0.152e-10
$\tau_{ACBranch}$	1.572	0.492e-01	1.297	0.400e-01	1.434
ε_{HTP}	0.535e-02	0.288e-03	0.509e-02	0.286e-03	0.522e-02
ε_{Branch}	0.409e-02	0.167e-01	0.421e-02	0.235e-03	0.415e-02
Objective Function	1.233		1.226		1.230

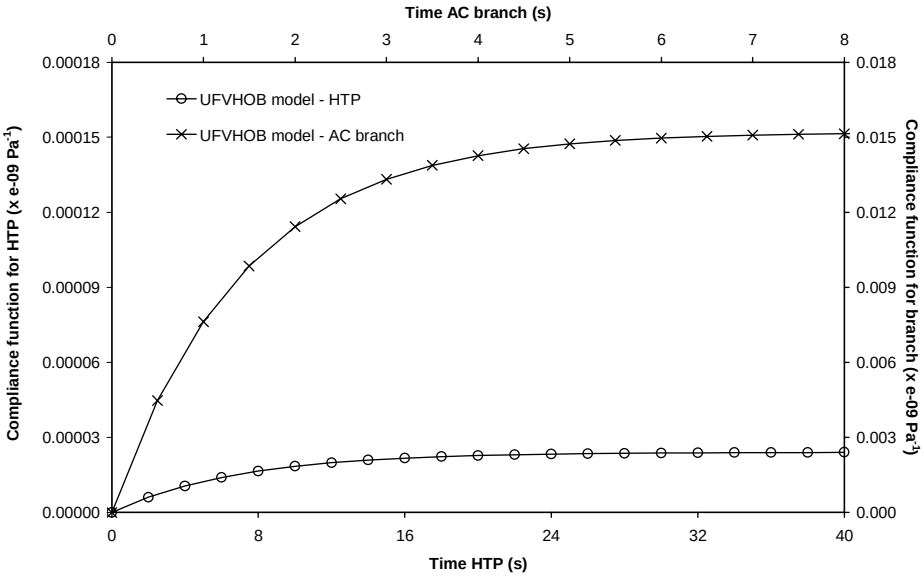

Figure 8-40 – Compliance function curves for HTP and AC (offtake) branch following calibration of the UFVHOB model using long term measured responses

Figures 8-41 and 8-42 show the comparison, at station 1, between measured and predicted responses for test 1, after calibrating using the UFVHOB model and long

term measured response, presented over 580s and 100s, respectively. The calibration gives an average objective function of 1.230. Figure 8-42 shows that, as for the other calibration models, the measured dispersion over the initial response is not replicated in the predicted response. This is a consequence of the calibration being dominated by the long term information in the measured response at the expense of accuracy over the short term.

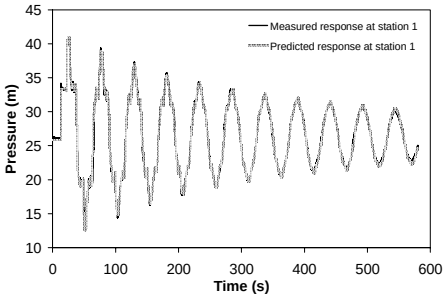

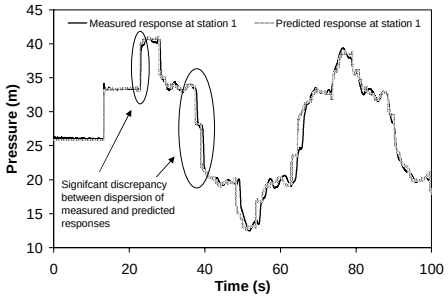

Figures 8-41 and 8-42 - Measured and predicted responses obtained using the UFVHOB model calibrated to long term response, over 580s and 100s, respectively

8.5.4 Calibration of UFVHOB model over 2L/a seconds

Table 8-10 shows the results of the calibration for tests 1 and 2, using short term measured responses, when the unsteady friction with a uniformly distributed "viscous" effect along the Hanson Transmission Pipeline and offtake branch (UFVHOB) model is applied. The average fitted roughness values, for tests 1 and 2, were 3.69mm and 5.68mm for the Hanson Transmission Pipeline (HTP) and offtake branch, respectively. Significantly, the fitted roughness for the HTP is closer to the known value for the calibration using the short term measured responses.

The calibrated value for parameter J_{HTP} varies from 0.241e-13 Pa^{-1} to 0.158e-11 Pa^{-1} for the long and short term calibrations, respectively. That said, and in contrast to the situation for entrained air, the use of two distinct calibrated values (i.e., those from the long and short term calibrations), at different stages of the transient response, is plausible. The inconsistency between the "viscous" damping calibrated over the initial and later stages of the measured responses may be physically explained if the

magnitude of the "viscous" damping is frequency dependent (i.e., if mechanical dispersion and damping are disproportionately greater over the initial stages of the transient response of the HTP relative to the later stages).

Table 8-10 - Fitted HTP and offtake branch roughness values, and "viscous" parameters, obtained by calibrating an UFVHOB model over the short term

Fitted Parameter	TEST 1		TEST 2		Average Value of Mean μ
	Mean μ	Standard Deviation σ	Mean μ	Standard Deviation σ	
J_{HTP}	0.152e-11	0.426e-13	0.164e-11	0.453e-13	0.158e-11
τ_{HTP}	0.100	0.111e-01	0.103	0.110e-01	0.102
$J_{ACBranch}$	0.138e-10	0.253e-11	0.112e-10	0.300e-11	0.125e-10
$\tau_{ACBranch}$	6.574	2.087	6.927	2.286	6.751
ε_{HTP}	0.386e-02	0.176e-02	0.352e-02	0.121e-02	0.369e-02
ε_{Branch}	0.542e-02	0.356e-02	0.594e-02	0.303e-02	0.568e-02
Objective Function	0.207		0.193		0.200

Figure 8-43 shows the comparison of the compliance function curves for the HTP based on the J_{HTP} parameters obtained for the long term and short term calibrations. The "viscous" damping acts much earlier and with greater magnitude in the case of the short term relative to long term calibration. This suggests that the action of the mechanical dispersion and damping may be more dominant over the early stages of the transient response (i.e., when high frequency content of the transient response is still significant).

Figures 8-44 and 8-45 show the comparison between measured and predicted responses for test 1, after calibration of the UFVHOB model over the short term, at stations 1 and 2, respectively. The calibration gives an average objective function of 0.200. This value is significantly lower than that achieved for the corresponding long term calibration. However, the insets in Figures 8-44 and 8-45 show that the structure of the wavefront reflected from the closed butterfly valve at "Sheep Dip" (for example) is not accurately replicated.

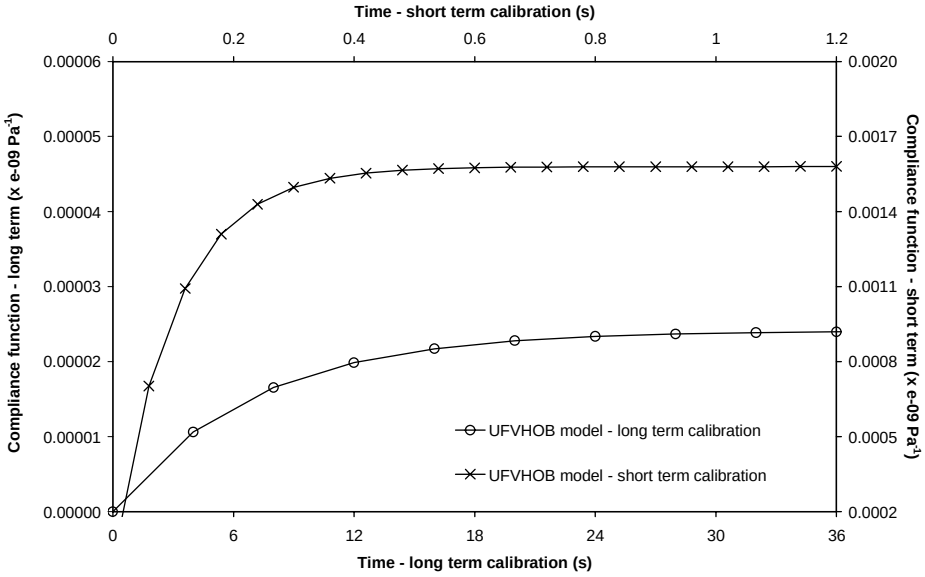

Figure 8-43 – Comparison of compliance function curves obtained for HTP following calibration using the UFVHOB model over the long and short term, respectively

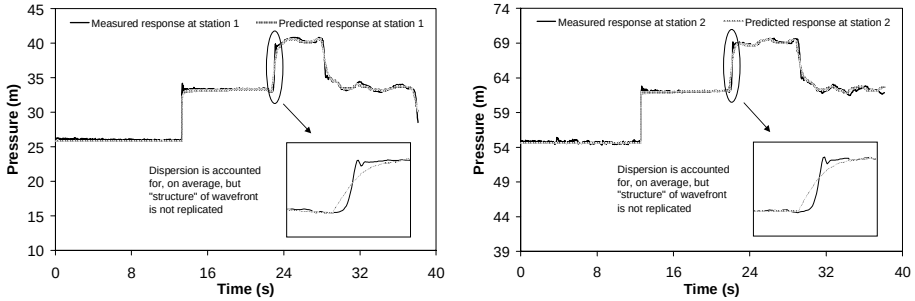

Figures 8-44 and 8-45 – Measured and predicted responses for test 1 obtained using the UFVHOB model calibrated over the short term, at stations 1 and 2, respectively

The use of equivalent "viscous" damping is an approximate method for replicating the effects of mechanical dispersion and damping and cannot be used to replicate the structure of measured wavefronts (because it does not replicate the fundamental physical processes). Unfortunately, neither the physical models developed by Skalak (1956) nor Budny et al. (1991) can account for the observed dispersion. Furthermore, the variable effects of restraints defy practical definition even under controlled laboratory conditions. This is why Williams (1977) and Budny et al. (1991) resorted

to the use of the equivalent “viscous” damping models that are commonly applied to describe other engineering phenomena with complex energy loss mechanisms.

8.5.5 Regression results for UFVHOB model

The average coefficient of determination is 98.0%, for both tests 1 and 2, following calibration using long term measured responses (580 seconds) and the unsteady friction and “viscous” Hanson pipeline and offtake branch (UFVHOB) model. The average coefficient of determination is 99.6%, for both tests 1 and 2, following calibration using short term measured responses (2L/a seconds). The lower coefficient for the long term relative to short term calibration confirms the observation that the long term calibration does not account for the dispersion in the measured responses with the same accuracy as the short term calibration over the initial stages of the transient responses.

Figures 8-46 and 8-47 show the standardised residual plotted against time, for the calibration performed using the long term measured responses, for test 1, at station 1, over time periods of 580s and 100s, respectively. As for the results obtained using the other calibration models, calibrated using long term measured responses, a lag between the measured and predicted response is discernable as a series of spikes over, in particular, the initial 100s of the response.

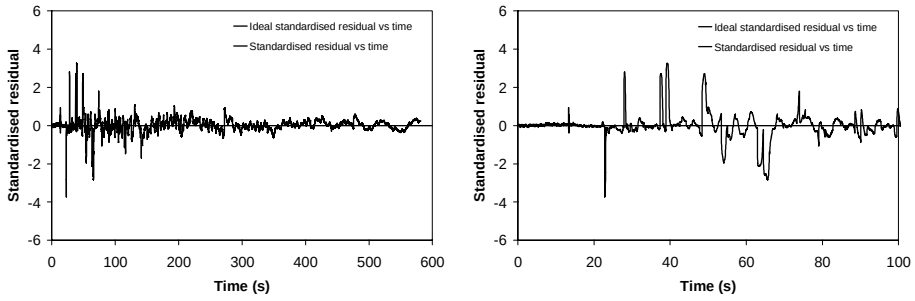

Figures 8-46 and 8-47 – Standardised residual versus time plots obtained using the UFVHOB model, calibrated over the long term, over 580s and 100s, respectively

Figures 8-48 and 8-49 show the standardised residual plotted against time, for the calibration performed using the short term measured responses, for test 1, at stations 1 and 2, respectively. The spikes apparent for the other models calibrated over the long term are no longer apparent although small discontinuities persist where there are discrepancies between the sharpness of the measured and predicted wavefronts.

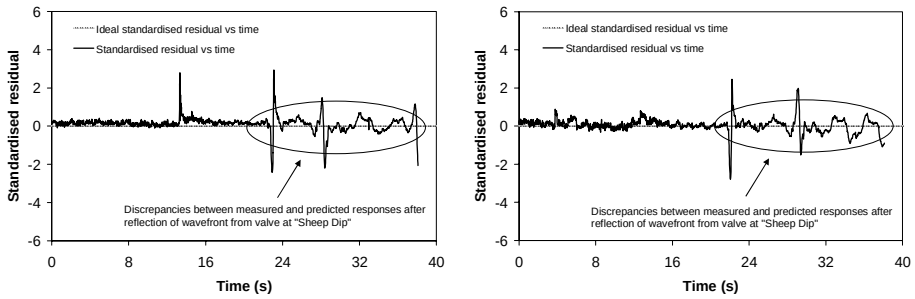

Figures 8-48 and 8-49 - Standardised residual versus time plots for UFIHOB model calibrated over the short term for test 1, at stations 1 and 2, respectively

8.5.6 Parameter correlations for long and short term calibrations

Table 8-11 shows the correlations, for test 1, between the parameters obtained using the unsteady friction and "viscous" Hanson pipeline and offtake branch (UFVHOB) model calibrated over the long term. The parameters are either weakly or moderately correlated except for J_{HTP} and the roughness for the offtake branch (which are strongly correlated). Prime facie, the lack of strong correlation between J_{HTP} and the roughness along the main pipeline suggests that both parameters can be independently calibrated using only measured pressure responses.

Table 8-12 shows the correlations, for test 1, between the parameters obtained using the UFVHOB model calibrated over the short term. In contrast to the results obtained using the other calibration models, the roughness for the HTP and the offtake branch are highly correlated with parameters J_{HTP} and τ_{FTP}. There is a lack of correlation between parameters J_{HTP} and $J_{AC\ Branch}$, and parameters τ_{FTP} and $\tau_{AC\ Branch}$.

Table 8-11 - Correlation of "viscous" parameters, and HTP and offtake branch roughness, for UFVHOB model calibrated over the long term

	J_{HTP}	τ_{HTP}	J_{BRANCH}	τ_{BRANCH}	ε_{HTP}	ε_{BRANCH}
J_{HTP}	1.000	0.092	-0.735	-0.524	-0.419	0.987
τ_{HTP}	0.092	1.000	-0.207	0.025	-0.232	0.064
J_{BRANCH}	-0.735	-0.207	1.000	-0.179	0.172	-0.740
τ_{BRANCH}	-0.524	0.025	-0.179	1.000	0.443	-0.498
ε_{HTP}	-0.419	-0.232	0.172	0.443	1.000	-0.373
ε_{BRANCH}	0.987	0.064	-0.740	-0.498	-0.373	1.000

Table 8-12 - Correlation of "viscous" parameters, and HTP and offtake branch roughness, for UFVHOB model calibrated over the short term

	J_{HTP}	τ_{HTP}	J_{BRANCH}	τ_{BRANCH}	ε_{HTP}	ε_{BRANCH}
J_{HTP}	1.000	-0.986	-0.299	-0.451	-0.982	1.000
τ_{HTP}	-0.986	1.000	0.138	0.320	0.993	-0.988
J_{BRANCH}	-0.299	0.138	1.000	0.849	0.157	-0.290
τ_{BRANCH}	-0.451	0.320	0.849	1.000	0.344	-0.444
ε_{HTP}	-0.982	0.993	0.157	0.344	1.000	-0.984
ε_{BRANCH}	1.000	-0.988	-0.290	-0.444	-0.984	1.000

The correlation between the "viscous" damping (parameter J_{HTP}) and fitted pipe roughness along the main pipeline (parameter ε_{HTP}), and also along the offtake branch (parameter ε_{BRANCH}), is important. The correlation indicates that the dispersion and damping caused by mechanical motion and vibration cannot be readily separated, using only inverse calibration to measured pressure responses, for the calibration performed using short term measured responses. The correlation of pipeline roughness with "viscous" damping along the main pipeline is a significant problem if inverse transient calibration for the roughness of transmission pipelines is to be performed using only measured pressure response information. Further investigation of this problem is beyond the scope of this research and will require the interpretation of

additional information regarding the magnitude of mechanical dispersion and damping (possibly based on an assessment of reflections and oscillations in measured transient responses). As mentioned in Chapter 7, this work is currently being undertaken by the author in tests on other transmission pipelines.

8.6 Feasibility of fitted roughness values

8.6.1 Summary of calibrated roughness values

One of the South Australian Water Corporation's motivations for permitting the transient tests was to investigate a loss of hydraulic efficiency in the Hanson Transmission Pipeline (HTP). The evidence for this inefficiency was a loss of flow capacity, despite the maintenance of constant head, over a period of years. As documented in Appendix N, specific CCTV camera investigation was performed near the location of Gum Creek over a length of approximately 300m. This investigation revealed limited spalling and/or corrosion and confirmed an approximate roughness of 2mm. Hence, the source of the hydraulic inefficiency was not identified by direct investigation.

Table 8-13 summarises the roughness values for the HTP and offtake branch, obtained, for test 1, when the quasi-steady friction (QSF), unsteady friction (UF), discrete gas cavity with unsteady friction (DGCUF) and unsteady friction and "viscous" Hanson pipeline and offtake branch (UFVHOB) models are calibrated over the long term. The predicted steady state pressures corresponding to each of these roughness values, together with the predicted steady state pressures obtained with a fixed roughness of 2.0mm along the HTP and offtake branch, are listed. The average measured steady state pressures, over a period of 12.5s prior to the induction of the transient in the HTP, were 25.93m and 54.69m, at stations 1 and 2, respectively.

There is significant variation in the calibrated roughness for the HTP with the highest and lowest values of 6.98mm and 2.75mm obtained for the QSF and DGCUF models, respectively. The fact that the known roughness along the HTP is approximately 2mm, as confirmed by CCTV camera investigation and the measured steady state pressures, suggests that the inverse transient calibration performed using the DGCUF

model gives the most accurate estimate of roughness. That said, the entrained air model, calibrated using long term measured responses, does not satisfactorily replicate the dispersion of the observed wavefronts. Furthermore, calibration of the DGCUF over the long and short term gave inconsistent quantities of entrained air without any plausible physical explanation.

Table 8-13 – Summary of calibrated roughness values, for long term calibration, and measured and predicted steady state pressures

Calibration Model	ε_{HTP} (mm)	ε_{BRANCH} (mm)	Station 1			Station 2		
			Obs. (m)	Pred. (m)	$\Delta_{Obs-Pred}$	Obs. (m)	Pred. (m)	$\Delta_{Obs-Pred}$
All models	2.00 fixed	2.00 fixed	25.93	25.95	-0.02	54.69	54.71	-0.02
Quasi-steady friction (QSF) model	6.98	3.04	25.93	25.81	0.12	54.69	54.57	0.12
Unsteady friction (UF) model	6.51	3.98	25.93	25.82	0.11	54.69	54.58	0.11
Unsteady friction and entrained air (DGCUF)	2.75	3.38	25.93	25.94	-0.01	54.69	54.70	-0.01
Unsteady friction and "viscous" damping (UFVHOB)	5.22	4.15	25.93	25.86	0.07	54.69	54.62	0.07

Table 8-14 summarises the roughness values for the HTP and offtake branch, obtained, for test 1, when the UFVHOB model is calibrated over the short term. The roughness value for the HTP was 3.69mm. This value compares favourably with the known roughness value. By restricting the calibration to the measured response over the short term, the value of the "viscous" damping parameter J_{HTP} increases to replicate the dispersion over the initial stages of the transient responses. As a consequence, the calibrated roughness decreases.

Table 8-14 – Summary of calibrated roughness values, for short term calibration, and measured and predicted steady state pressures

Calibration Model	ε_{HTP} (mm)	ε_{BRANCH} (mm)	Station 1			Station 2		
			Obs. (m)	Pred. (m)	$\Delta_{Obs-Pred}$	Obs. (m)	Pred. (m)	$\Delta_{Obs-Pred}$
Unsteady friction and "viscous" damping (UFVHOB)	3.69	5.68	25.93	25.88	0.05	54.69	54.64	0.05

8.6.2 Use of steady state pressures to assess calibrations

Despite the variation in the calibrated roughness values for the Hanson Transmission Pipeline (HTP) and the offtake branch, the predicted steady state pressures only range between 25.81m to 25.90m and 54.57m to 54.66m at stations 1 and 2, respectively. That said, the steady state information provides a valuable gauge of the roughness along the HTP and between stations 1 and 2. Increasing the flow rate along the HTP and offtake branches would have also increased the sensitivity of the steady state response to the roughness values. Unfortunately, these tests were beyond the scope of this research and could not be scheduled with the South Australian Water Corporation. Nevertheless, the information from the CCTV camera investigation is corroborated by the minimisation of the difference between the measured and predicted steady state pressures when the roughness values are in the range of 2mm and confirms, rather than contradicts, the magnitude of roughness estimated from the CCTV camera footage.

8.7 Summary

The effects of phenomena such as unsteady friction, entrained air and mechanical dispersion and damping on the accuracy, or feasibility, of roughness calibration of transmission pipelines using inverse analysis has not been previously investigated. Furthermore, the tests presented in this research have revealed that these phenomena are significant, to varying degrees, in the field. Increasingly complex forward transient models have been presented in this chapter and then calibrated, using inverse analysis, to obtain estimates of key model parameters. Regression diagnostics,

including the coefficient of determination for the calibrated predicted response, standardised residuals and parameter correlations, have been examined to assess structural model errors and the robustness of calibrated parameters.

Quasi-steady friction (QSF), unsteady friction (UF) and discrete gas cavity with unsteady friction (DGCUF) models have been calibrated to the measured responses from the Hanson Transmission Pipeline (HTP) for tests 1 and 2 without any artificially introduced fault(s). The calibrated roughness of the HTP obtained using the QSF and UF models was found to significantly exceed the known roughness value of approximately 2mm. This was despite considerable improvement in the inverse fit (objective function) when the algorithms for unsteady friction were applied. This confirmed that an improvement in objective function does not necessarily mean that the structure of, or the estimated parameters derived from, postulated models are physically accurate. The DGCUF model was developed to determine whether entrained air could account for significant dispersion observed in the measured responses. Both the roughness of the HTP and a distributed volume of entrained air were simultaneously calibrated using long term measured responses and the DGCUF model. However, the volume of entrained air, calibrated using the long term measured responses, did not account for the observed dispersion. The calibration was restricted to the first 2L/a seconds to determine whether the dispersion could be modelled over the short term only. While the observed dispersion was better modelled, the volume of entrained air calibrated over the short term was significantly greater than that calibrated over the long term and this physical inconsistency could not be explained.

Mechanical dispersion and damping caused by motion and vibration at restraints was suspected. Numerous gullets (underground sections), bends, cross-connections, valve chambers and other variable restraints were identified. Extending the laboratory findings of Williams (1977) and Budny et al. (1991), a “viscous” dispersion and damping calibration mechanism has been included in an unsteady friction and “viscous” Hanson pipeline and offtake branch (UFVHOB) model. The UFVHOB was calibrated using long and short term measured responses. As for the DGCUF model, the long term calibration was unable to replicate observed dispersion over the initial stages of the measured responses. The short term calibration better replicated the initial dispersion of the observed wavefronts. The “viscous” dispersion and damping

parameters for the long and short term calibrations were inconsistent. However, this inconsistency was feasible providing the mechanical dispersion and damping affecting the HTP is frequency dependent.

While the UFVHOB model is plausible, and improves the accuracy of the calibrated forward transient model, the correlation between the calibrated roughness of the HTP and the "viscous" damping parameter, which were simultaneously calibrated, was relatively strong for the short term calibration. The influence of friction and "viscous" damping were therefore not independent during the calibration. This means that measured pressure responses are not sufficient to facilitate independent inverse calibration of model parameters representing the effects of friction and mechanical dispersion and damping (at least for the calibration of the UFVHOB model over the short term). Additional information or model complexity is therefore required to separate the effects of fluid and mechanical friction.

The feasibility of the calibrated roughness of the HTP was checked against available CCTV camera steady state flow and pressure information revealing that the DGCUF model gave the most realistic roughness values. The UFVHOB model gave the next most realistic estimate (however, a roughness of 5.22mm is significantly greater than the known roughness value of approximately 2mm). Overall, a more comprehensive understanding of the respective contributions of fluid friction, entrained air and mechanical dispersion and damping is required before inverse transient calibration for transmission pipeline roughness can be improved. That said, Inverse Transient Analysis (ITA) for leak detection on the HTP will be attempted in Chapter 9 using the QSF, UF and UFVHOB models developed in this chapter.